Investigation of Vortex Patterns on Slender Bodies at High Angles of Attack

Wu Genxing,* Wang Tzehsing,† and Tian Shixhong‡
Nanjing Aeronautical Institute, Nanjing, China

The method of the fluorescent minituft has been used to investigate experimentally the changes of the spatial vortices with angle of atttack and without sideslip on the lee side of some slender bodies in a low-speed tunnel. Top and side views of the vortex have been acquired. The axial velocities and the circulation of the vortex along its track were measured for symmetric and asymmetric vortex patterns on a sharp ogive body of revolution. Hot-wire anemometer and fluorescent minituft were used to measure the velocities and circulation, respectively. It is shown that the vortex pattern on these slender bodies is similar. Also the model of the asymmetric vortex and the interference between the vortices are realized to some extent. The vortex track near the rear of the body is almost unaffected by the presence of a small protrusion at the fore part of the sharp body of revolution for a symmetric vortex pattern at larger angle of attack. As for an asymmetric vortex pattern, it can strongly affect the vortex track.

Introduction

IT is necessary for modern aircraft and missiles to fly at large angles of attack in order to obtain high maneuverability. With increasing angle of attack, the vortex patterns on the lee side of slender bodies become asymmetric even without sideslip. The asymmetric vortices produces an undesirably large side force and yawing moment. Most research has been directed toward the study of the effects of geometric parameters of the body, the Reynolds number, and the roll angle of the model, etc., on the side force. Also, some methods for reducing the side force have been studied.[1-7] Some researchers have measured the pattern and circulation of the vortex at a few cross sections,[8-10] while others have acquired the side view of the vortex track by schlierengraph.[11] The top view of the vortex track has yet to be shown.

The objective of the present study is to measure the change of spatial vortex tracks with angles of attack without sideslip on the lee side of some slender bodies in a low-speed tunnel. The method of the fluorescent minituft is used so that the vortex pattern can be recorded in more complete detail. Top and side views of the vortex tracks have been acquired. Four different slender bodies are studied in order to illustrate the effect of the geometry of the body on the vortex pattern. The axial velocity of the vortex core measured with the hot-wire anemometer and the circulation of the vortex measured by the method of the fluorescent minituft along the vortex tracks are given for the symmetric and asymmetric vortex pattern on a sharp ogive body of revolution so that the character of the spatial vortex can be clearly understood. The effects of a small protrusion at the fore part of the slender body on the vortex tracks are also investigated. Surface oil flow is used in order to compare it with vortex tracks.

Models and Experiment

The vortex tracks were measured in a 0.75×0.75-m low-speed wind tunnel at a velocity of 30 m/s. The Reynolds number was about 1.2×10^5 (based on the diameter), which produced laminar boundary-layer separation. The angle of attack of the models was varied from 10-60 deg. The axial velocity of the vortex center and the circulation of the vortex were measured in the 1.5×1.5-m low-speed wind tunnel. The large model was twice as long as the small model. The test Reynolds number was about 1.6×10^5.

Figure 1 shows the shape of four slender bodies of different cross sections. The fineness ratio of the forebody and the cylindrical afterbody was 3.5. Models A and B were sharp or blunted bodies of revolution with the forebody of a tangent ogive. Models C and D were sharp slender bodies with horizontal or vertical elliptical cross-section shape.

The method of the fluorescent minituft is used to measure the tracks and the circulation of the spatial vortex.[12] The fluorescent minituft is made of nylon filament. Its diameter is about .02 mm. When it was immersed in the vortex flow, its rotational speed was measured by a nitrogen molecule laser, so the circulation of the vortex calculated. The spatial vortex track was recorded by the camera. The coordinate of the vortex track and the circulation of the vortex were normalized by the length of the model L and the maximum circulation Γ_{max} along the vortex track.

Results and Discussion

Effect of Angle of Attack

The change of the vortex tracks with angle of attack on the sharp body of revolution can be divided into stages.

The vortex pattern is symmetric. For angles of attack less than 12 deg, there is attached flow in the front of the body. However, there are two symmetric primary vortices in the rear of the body (see Fig. 2). The point at which the symmetric vortex originates moves from the base to the tip of the body with increasing angle of attack. For angles of attack from 12-30 deg, two symmetric vortices originate from the apex of the body and extend to the base of the body on the lee side. The vortex tracks are above the cylinder and nearly parallel to the axis of the body, as shown in Fig. 3. It can also be shown that the axial velocities and the circulation of the two symmetric vortices are equal and increase along the vortex track as shown in Fig. 4. Besides a pair of primary vortices, a pair of second vortices with the same rotational direction as that of the primary vortices is positioned near the separation line. This pair is different from the primary pair, which is fed by a sheet of vorticity from the surface. According to the surface oil flow and the measurement of vortex tracks, the cross-flow stream lines would be as shown

Received April 12, 1985; revision received Oct. 28, 1985.

*Lecturer, Department of Aerodynamics.
†Senior Engineer, Department of Aerodynamics.
‡Research Assistant, Department of Aerodynamics.

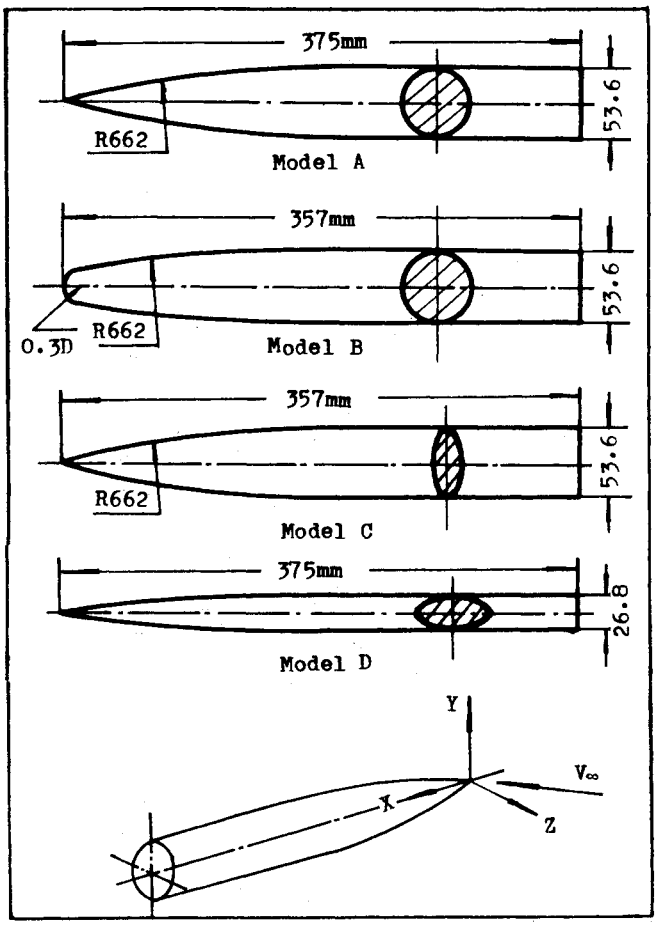

Fig. 1 Model and coordinate system (model A, sharp body of revolution; model B, blunt body of revolution; model C, sharp slender body with horizontal elliptical section; model D, sharp slender body with vertical elliptical section).

in Fig. 5. The second vortex is a pair of interior vortices (interior focus). There is still a pair of secondary vortices induced by the primary vortex as shown in the test of the oil flow. Their rotational direction to each is opposite to the corresponding primary vortex. Its core is smaller than the primary vortex. The primary and the second vortex move away from the body and their cores increase in size with increasing angle of attack. The second and secondary vortices are usually negligible.

According to the impulsive-flow analogy, flow over a two-dimensional cylinder at successive instants can translate into flow over a slender body with an equivalent axial cross section. When the angle of attack becomes greater than 30 deg, the circulation and the position of the symmetric vortex at the base of the body become unsteady. The two primary vortices begin to become asymmetric under the effect of disturbances similar to the flow pattern of a cylinder starting from rest.[13] One of them is lower, while the other, higher vortex is slightly turned up near the base of the body. Because of the inductive effect between them, the lower vortex is nearer the symmetric plane of the body, while the higher one bends farther away (see Fig. 6). Therefore, side forces are generated. With increasing angle of attack, the asymmetric phenomenon becomes larger and moves forward. The rear of the higher vortex gradually begins to turn parallel to the freestream. As the primary vortices turn, the second vortices also begin to move away from the body.

The change in axial velocity and circulation of the vortex at a 45-deg angle of attack are given in Fig. 7. It can be shown that when the vortices turn up, the axial velocity and the circulation of the vortex begin to decrease. The vortex gradually

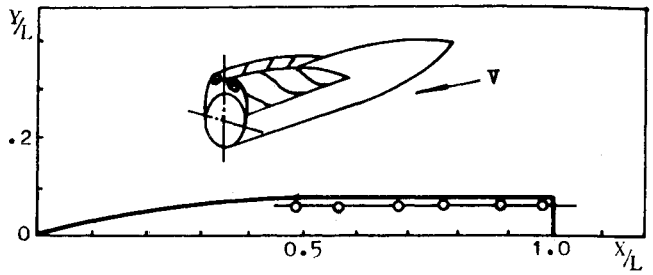

Fig. 2 The vortex track for the sharp body of revolution at angle of attack of 10 deg.

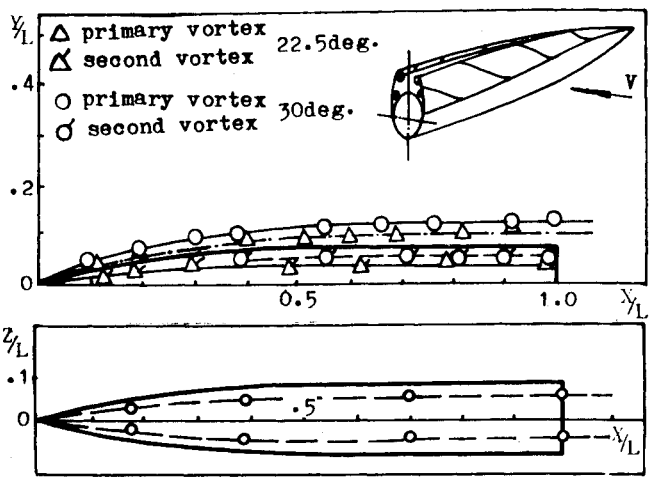

Fig. 3 The vortex track for the sharp body of revolution at angle of attack of 22.5 and 30 deg.

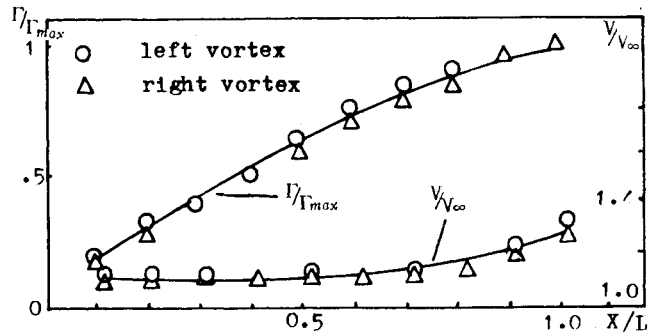

Fig. 4 The axial velocity and the circulation of the vortex for the sharp body of revolution at angle of attack of 22.5 deg.

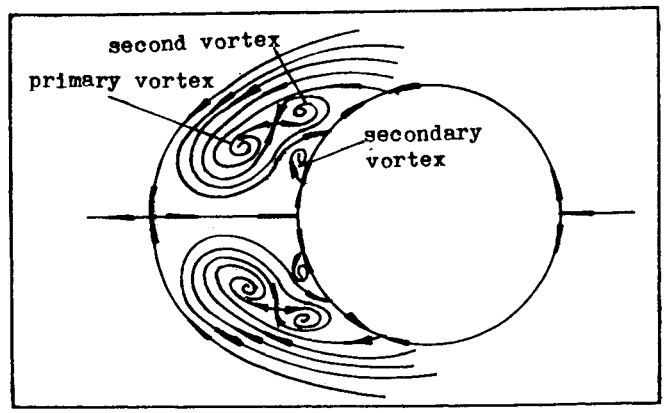

Fig. 5 The cross-flow streamlines (at $x/L = 0.9$) at angle of attack of 22.5 deg.

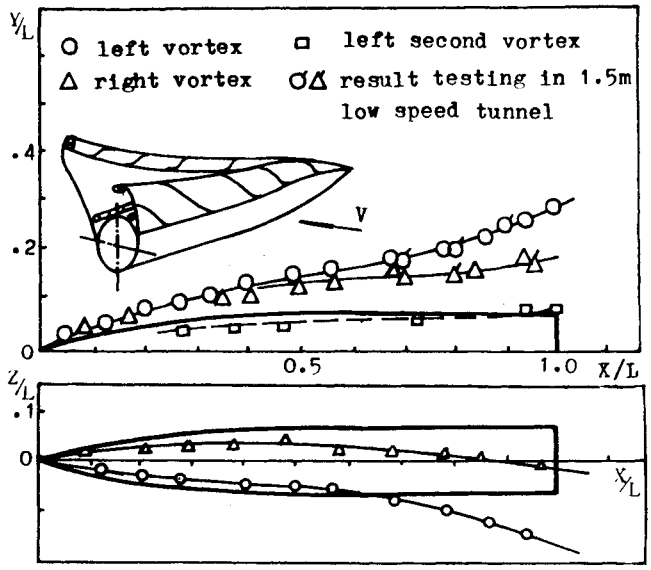

Fig. 6 The vortex track for the sharp body of revolution at angle of attack of 45 deg.

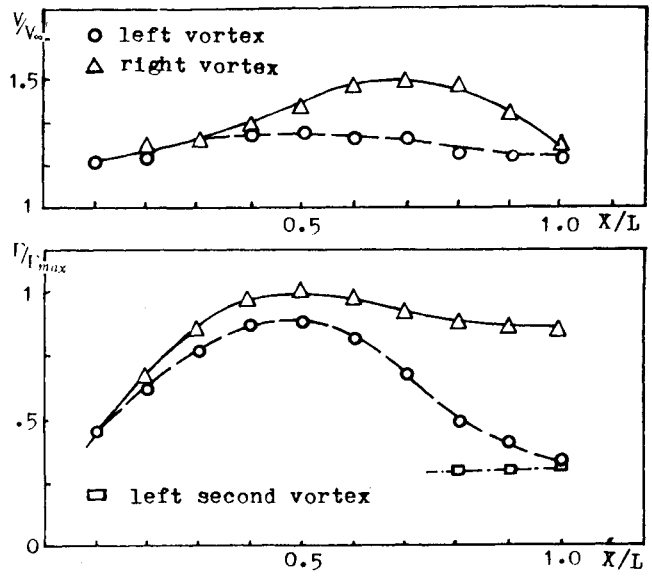

Fig. 7 The axial velocity and the circulation of the vortex for the sharp body of revolution at angle of attack of 45 deg.

begins to shed from the body and becomes a free vortex. The separated vortex around the circular cylinder no longer feeds into the turned-up vortex but does feed into the second vortex. The second vortex circulation is increased and it gradually becomes the second primary vortex, whose effect cannot be neglected. Comparison of the axial velocity and the circulation of the two vortices indicates that if the vortex tracks are symmetric, the axial velocity and the circulation are approximately equal on the forebody ($x/L<0.5$). The vortex tracks are obviously asymmetric for $x/L>0.5$. Both the axial velocity and the circulation of the lower vortex are obviously larger than that of the higher one. The inductive effect of the lower vortex on the body is stronger than that of the higher one.

The maximum value of the circulation at an angle of attack of 45 deg is twice as large as at angle of attack of 22.5 deg. It can be shown that the circulation of the vortex increases with angle of attack.

For angles of attack greater than 47 deg, when the second vortex has become the second primary vortex, the asymmetric two-vortex pattern changes into an asymmetric three-vortex pattern, as shown in Fig. 8. Under the inductive effect of the primary vortex of the other side, the second primary vortex always turns toward the symmetric plane of the body. The primary vortex of the other side deflects away from the symmetric plane of the body. Therefore the asymmetric side force does not increase and begins to decrease. The maximum side force occurs at the stage at which the two primary vortices deflect most severely and the second vortex does not become the second primary vortex.

For angles of attack greater than 55 deg, when the second primary vortex has shed from the body, as mentioned above, a third primary vortex will occur under the second primary vortex. With increasing angle of attack, the point at which the vortex begins to turn up and deflect moves forward from the back to the tip of the body. At this time, vortex breakdown can appear in the rear of the body. For angles of attack greater than 70 deg, the concentrated vortex can be observed near the nose, but the rest of the body is immersed in a random wake region like the two-dimensional flow around the circular cylinder (see Figs. 9 and 10).

Effect of Bluntness and Body Cross Section

The process of change of the vortex track on these bodies is similar to that on a sharp body of revolution. However, the angle of attack at which the various vortex patterns appear is different, as listed in Table 1.

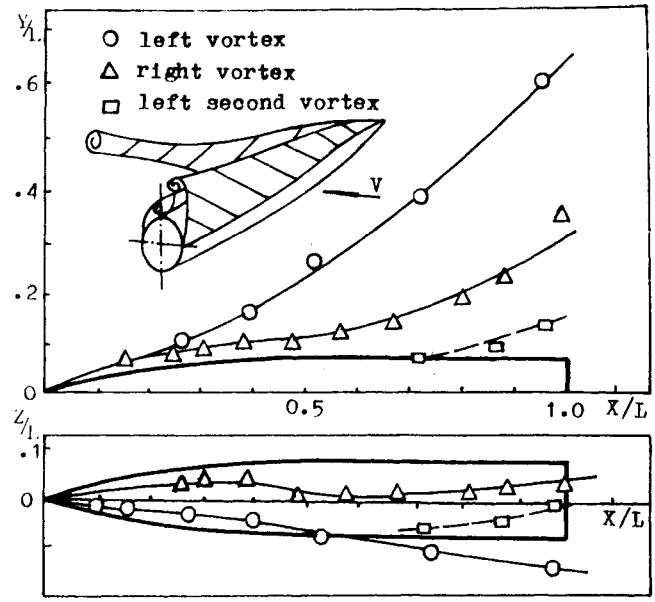

Fig. 8 The vortex track for the sharp body of revolution at angle of attack of 50 deg.

Table 1 The angle of attack for various vortex patterns

Vortex pattern	Angle of attack, deg			
	Model A	Model B	Model C	Model D
Partial symmetric	<12	<22	<10	<16
Whole symmetric	12-30	22-38	10-30	16-20
Two asymmetric	30-47	38-48	30-45	20-25
Three asymmetric	47-55	48-57	>45	>25

The particular characteristics are:

1) For a blunted body of revolution the change of the partial symmetric vortex pattern into the whole symmetric vortex pattern is delayed owing to the effect of flow around the blunt head. The angles of attack at which the two and three asymmetric vortex patterns occur are delayed. Comparison of Figs. 6 and 11 indicates that the vortex deflection generated on the blunt body of revolution is more moderate than it is on the sharp body of revolution. Therefore the asymmetric side force

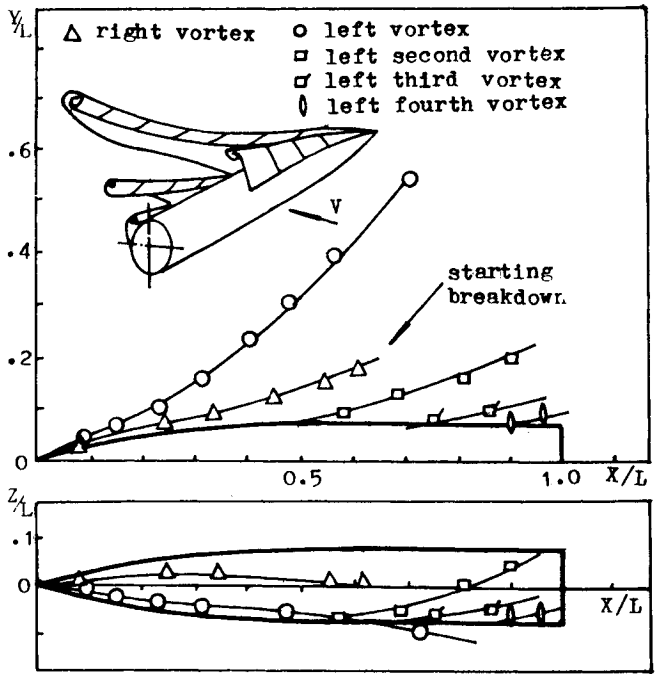

Fig. 9 The vortex track for the sharp body of revolution at angle of attack of 55 deg.

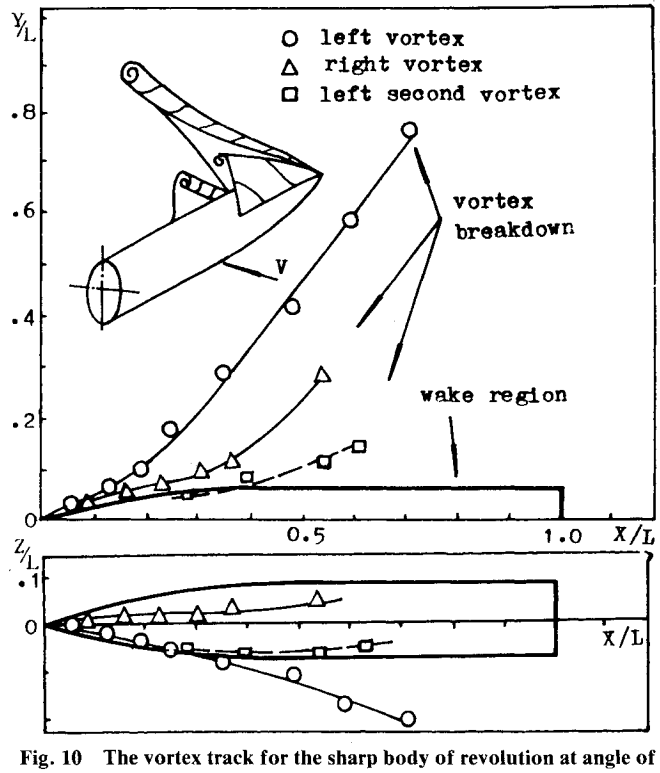

Fig. 10 The vortex track for the sharp body of revolution at angle of attack of 60 deg.

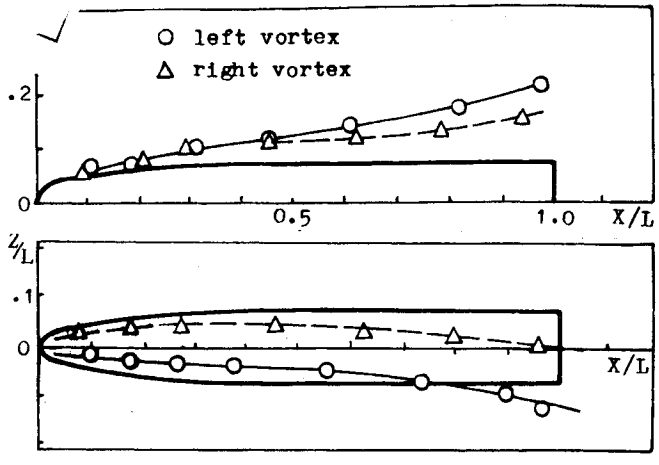

Fig. 11 The vortex track for the blunt body of revolution at angle of attack of 45 deg.

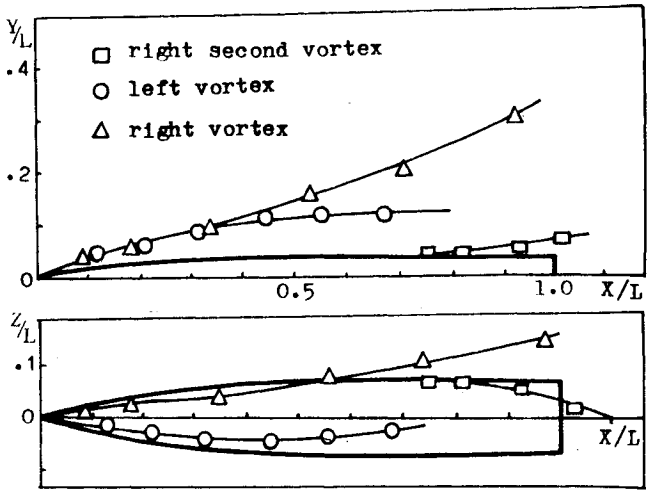

Fig. 12 The vortex track for the sharp slender body with horizontal elliptical section at angle of attack of 50 deg.

on the blunt body of revolution is less than that on the sharp body of revolution.

2) The sharp slender body with horizontal elliptical cross section and the sharp body of revolution have the same shape of projection. The angles of attack at which the various vortex patterns appear are approximately equal, but only the three asymmetric vortex pattern appears. For angles of attack greater than 50 deg, vortex breakdown appears in the rear of the lower primary vortex, as shown in Fig. 12. Therefore, before the third vortex takes place, the rear of the body becomes immersed in the random wake region. As angle of attack increases, the high and the low vortex change alternatively in the two asymmetric vortex pattern. For example, for an angle of attack of 30 deg, the right vortex is higher than the left vortex while, at an angle of attack of 40 deg, they are reversed.

3) For the sharp slender body with vertical elliptical cross section, the asymmetric two vortex pattern will appear soon after the whole symmetric vortex pattern is formed. The vortex pattern is shown in Fig. 13.

Effects of a Disturbance

A small protrusion, whose height and area are about 1/50 of the diameter and 0.5% of the cross-sectional area of the model, was set on the fore part of the sharp body of revolution in order to study the effect of a disturbance on the spatial vortex track. The disturbance affects only its downstream track. It was found that, for the symmetric vortex pattern, the downstream local track will move down due to the disturbance; however, the vortex track near the rear of the body is hardly affected, as shown in Fig. 14.

As for the asymmetric vortex pattern, if the protrusion is set to the side of the higher vortex, it affects its track strongly; while the effect on the lower vortex of the other side is smaller, as shown in Fig. 15. Comparison of Figs. 6 and 15 indicates that the vortex track has been reversed to its original form without the protrusion. Therefore, the side force is reversed. It

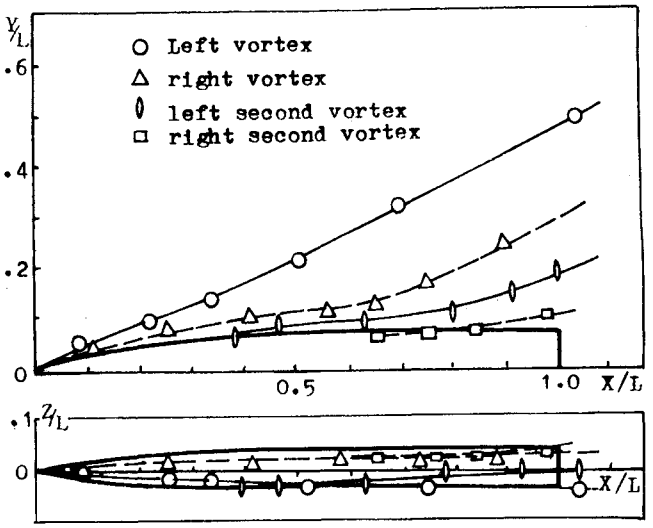

Fig. 13 The vortex track for the sharp slender body with vertical elliptical section at angle of attack of 30 deg.

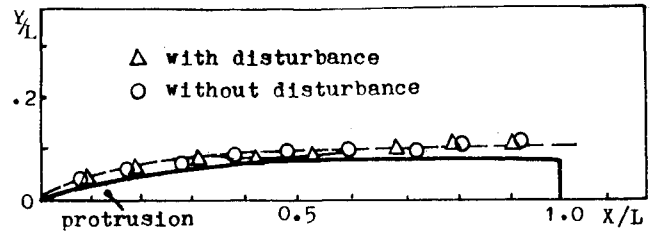

Fig. 14 The effect of a protrusion on the vortex track for the sharp body of revolution at angle of attack of 22.5 deg.

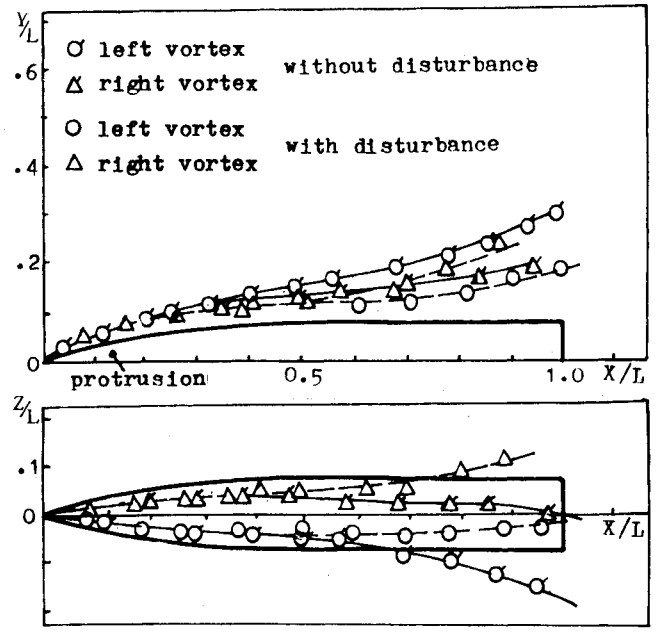

Fig. 15 The effect of a protrusion on the vortex track for the sharp body of revolution at angle of attack of 45 deg.

can be illustrated that the symmetric vortex pattern is more stable before it begins to become unsteady, since it seems to be able to absorb the disturbance. However, the asymmetric vortex pattern seems less stable. Once there is a disturbance, it can change its track immediately. The problems of vortex stabilization have to be studied further.

Conclusions

1) The development of the vortex track for the sharp body of revolution is as follows: partial symmetric vortex pattern ($\alpha < 12$ deg), whole symmetric vortex pattern ($\alpha < 30$ deg), asymmetric two vortex pattern ($\alpha < 47$ deg, the asymmetric side force is maximum in this range), asymmetric three vortex pattern ($\alpha < 55$ deg, the side force begins to decrease), asymmetric multiple vortex pattern ($\alpha < 60$ deg), and asymmetric vortex plus the random wake.

2) There are some particulars for slender bodies of different shape. For example, the angle of attack at which the asymmetric vortex pattern occurs is delayed and the vortex deflection is more moderate for the blunt body of revolution. However, the asymmetric vortex pattern can appear earlier and is similar to that of the von Kármán street for the sharp slender body with vertical elliptical section. Models A and C have the same shape of projection; the angles of attack at which the various vortex patterns appear are approximately equal.

3) Besides the pair of primary vortices, there is both a second vortex pair and a secondary vortex pair whose rotational direction is the same and opposite to that of the primary vortex, respectively. When the primary vortex has shed from the body and become the free vortex, the second vortex becomes a second primary vortex.

4) The vortex track near the rear of the body is almost unaffected by the protrusion for the symmetric vortex pattern before it begins to become unsteady. As for the asymmetric vortex pattern, the protrusion can strongly affect the vortex track.

References

[1]Keener, E.R., Chapman, G.T., Cohe, L., and Taleghani, J., "Side Forces on a Tangent Ogive Forebody with a Fineness Ratio of 3.5 at High Angles of Attack and Mach Numbers from 0.1 to 0.7," NASA TM X-3437, 1977.

[2]Kruse, R.L., Keener, E.R., and Chapman, G.T., "Investigation of the Asymmetric Aerodynamic Characteristics of Cylindrical Bodies of Revolution with Variations in Nose Geometry and Rotational Orientation at Angles of Attack to 58°and Mach Numbers to 2," NASA TM 78533, 1979.

[3]Ericsson, L.E. and Reding, J.P., "Vortex-Induced Asymmetric Load in 2-D and 3-D Flows," AIAA Paper 80-0181, Jan. 1980.

[4]Wardlaw, A.B. Jr. and Yanta, W.J., "The Flow Field About, and Forces on Slender Bodies at High Angles of Attack," AIAA Paper 80-184, Jan. 1980.

[5]Dexter, P.C. and Hunt, B.L., "The Effects of Roll Angle on the Flow over a Slender Body of Revolution at High Angles of Attack," AIAA Paper 81-0358, Jan. 1981.

[6]Lamont, P.J., "The Complex Asymmetric Flow over a 3.5D Ogive Nose and Cylindrical Afterbody at High Angles of Attack," AIAA Paper 82-0053, Jan. 1982.

[7]Yanta, W.J. and Wardlaw, A.B. Jr., "The Secondary Separation Region on a Body at High Angles of Attack," AIAA Paper 82-0343, Jan. 1982.

[8]Fidler, J.E., Schwind, R.G., and Niclsen, J.N., "An Investigation of Slender-body Wake Vortices," AIAA Paper 77-127, Jan. 1977.

[9]Oberkampf, W.L., Owen, F.K., and Shivanada, T.P., "Experimental Investigation of the Asymmetric Body Vortex Wake," *AIAA Journal,* Vol. 19, Aug. 1981.

[10]Wardlaw, A.B. Jr. and Yanta, W.J., "Multistable Vortex Patterns on Slender, Circular Bodies at High Incidence," *AIAA Journal,* Vol. 20, April 1982.

[11]Thomson, K.D. and Morrison, D.F., "The Spacing, Position and Strength of Vortices in the Wake of Slender Cylindrical Bodies at Large Incidence," *Journal of Fluid Mechanics,* Vol. 50, Pt. 4, 1971.

[12]Genxing, W. and Tzehsing, W., "The New Method Measuring the Position and Circulation of the Spatial Vortex in Low Speed Tunnel," *Proceedings of Flow Visualization and Its Applications,* Chinese Society of Mechanics, 1982.

[13]Perry, A.E., Chong, M. S., and Lim, T.T., "The Vortex Sheeding Process Behind Two Dimensional Bluff Bodies" *Journal of Fluid Mechanics,* Vol. 116, March 1982.